Hierarchical Nanostructuring of Porous Silicon with Electrochemical and Regenerative Electroless Etching

Ermei Mäkilä,[a] Anne-Mari Anton Willmore,[b] Haibo Yu,[c] Marianna Irri,[a] Mark Aindow,[c] Tambet Teesalu,[b] Leigh T. Canham,[d] Kurt W. Kolasinski,[e] and Jarno Salonen[a]

[a] Department of Physics and Astronomy, University of Turku, Turku, FI-20014, Finland

[b] Laboratory for Cancer Biology, University of Tartu, Tartu, 50411, Estonia

[c] Department of Materials Science & Engineering, Institute of Materials Science, University of Connecticut, Storrs, CT 06269-3136, USA

[d] School of Physics and Astronomy, University of Birmingham, Birmingham, B15 2TT, United Kingdom

[e] Department of Chemistry, West Chester University, West Chester, PA 19383-2115, USA

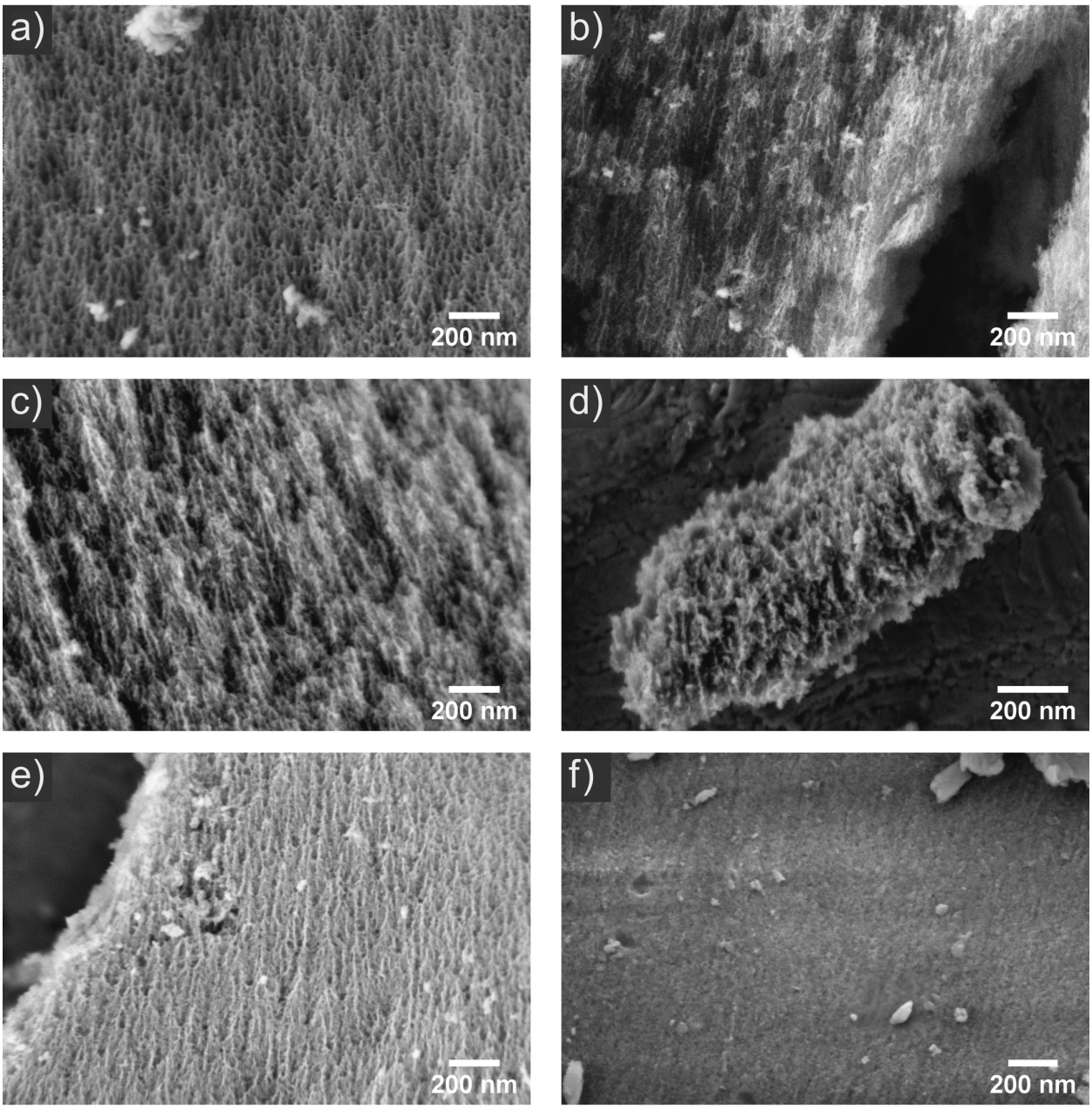

Figure S1. Secondary electron micrographs of the RaPSi samples (a) **1**, (b) **2**, (c) **4**, (d) **5**, (e) **7** and (f) **8**. The gross pore structure appears similar in all samples except **8**, which appears to have undergone structural collapse according to N_2 sorption results.

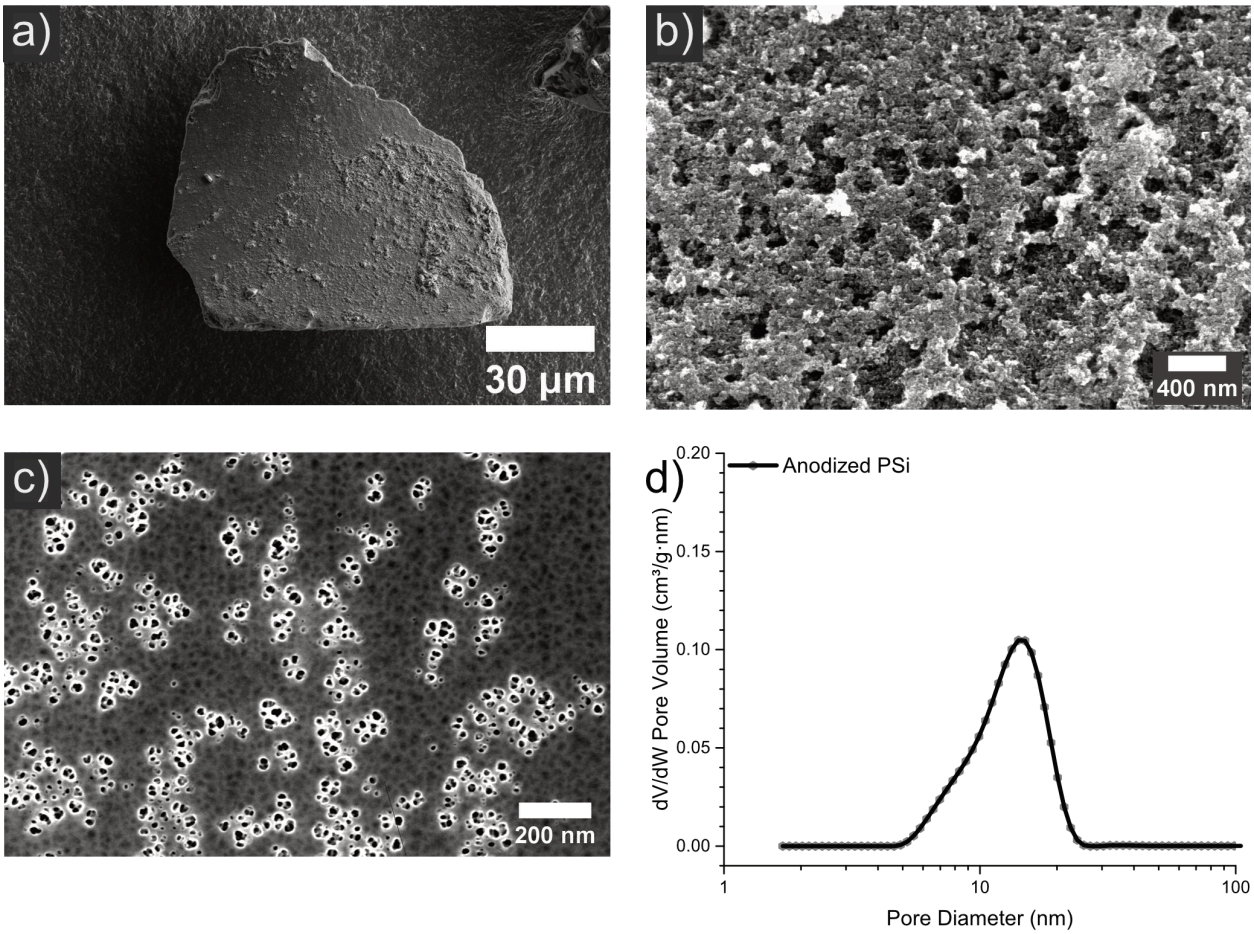

Figure S2.1. Representative SEM images obtained from an initial non-luminescent anodized PSi samples with specific surface area (SSA) of 286 ± 4 m^2/g and pore volume of 1.03 ± 0.01 cm^3/g with (a) overall image of an anodized PSi microparticle; (b) high magnification image from the surface of the particle and (c) high magnification image of the side wall of a FIB-cut slice through the particle. (d) Pore size distribution of the imaged anodized particles.

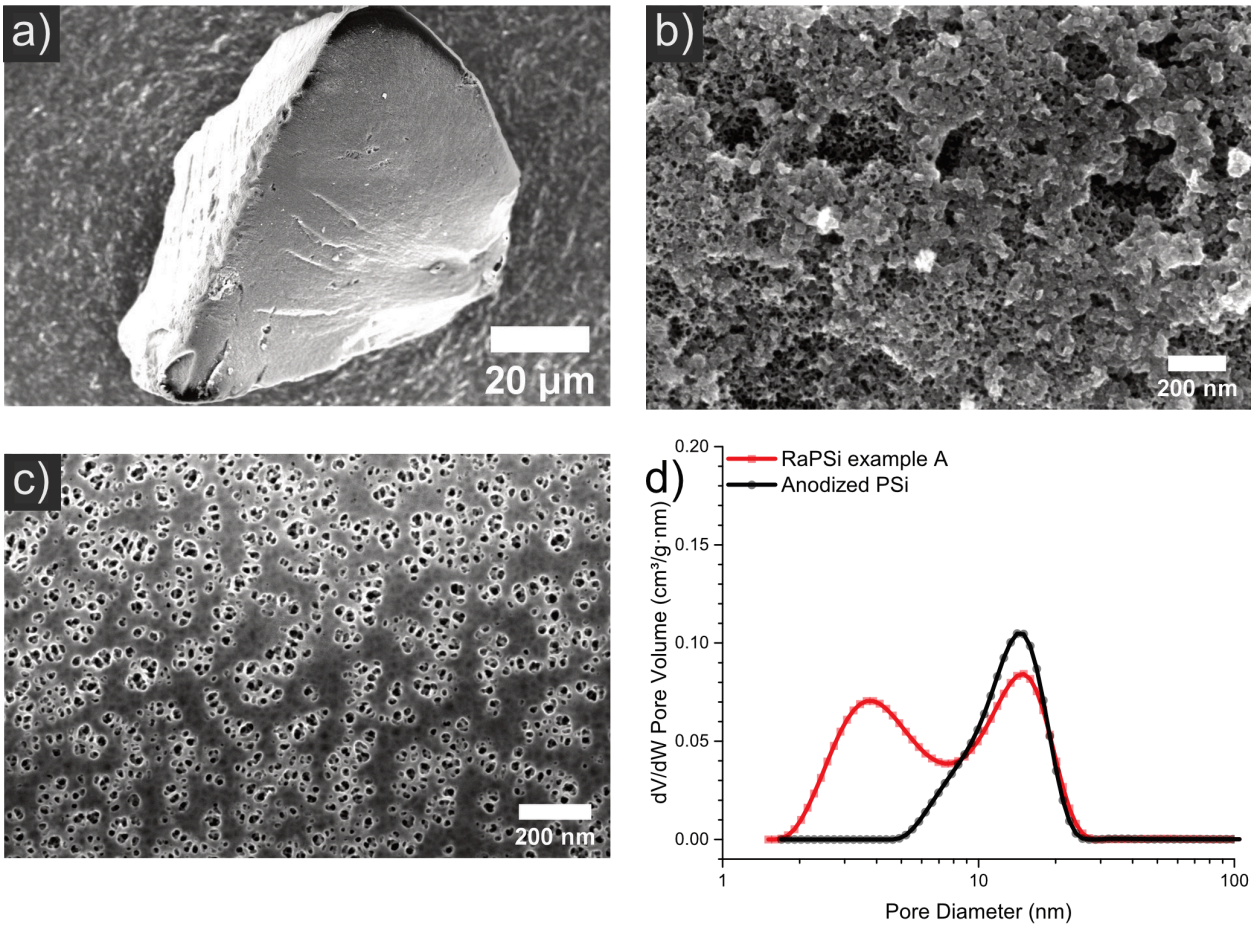

Figure S2.2. Representative SEM images obtained from a luminescent ReEtched, anodized PSi samples (RaPSi) with specific surface area (SSA) of 625 ± 3 m^2/g and pore volume of 1.20 ± 0.01 cm^3/g with (a) overall image of a RaPSi microparticle; (b) high magnification image from the surface of the particle and (c) high magnification image of the side wall of a FIB-cut slice through the particle. (d) Pore size distributions of the imaged RaPSi example particles with the respective initial anodized PSi.

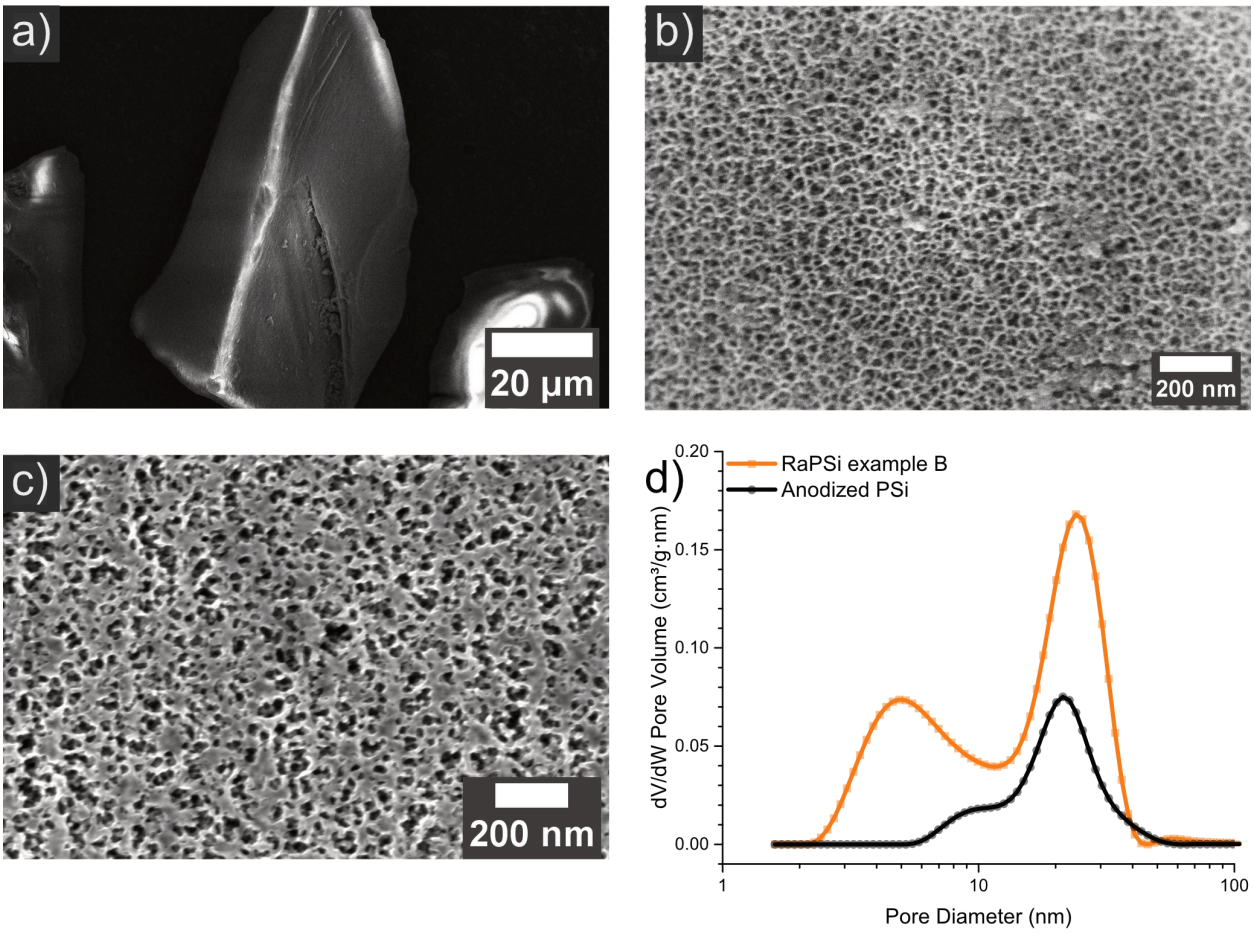

Figure S2.3. Representative SEM images obtained from a luminescent RaPSi samples with specific surface area (SSA) of 888 ± 3 m^2/g and pore volume of 3.20 ± 0.01 cm^3/g with (a) overall image of a RaPSi microparticle; (b) high magnification image from the surface of the particle and (c) high magnification image of the side wall of a FIB-cut slice through the particle. (d) Pore size distributions of the imaged RaPSi example particles with the respective initial anodized PSi.

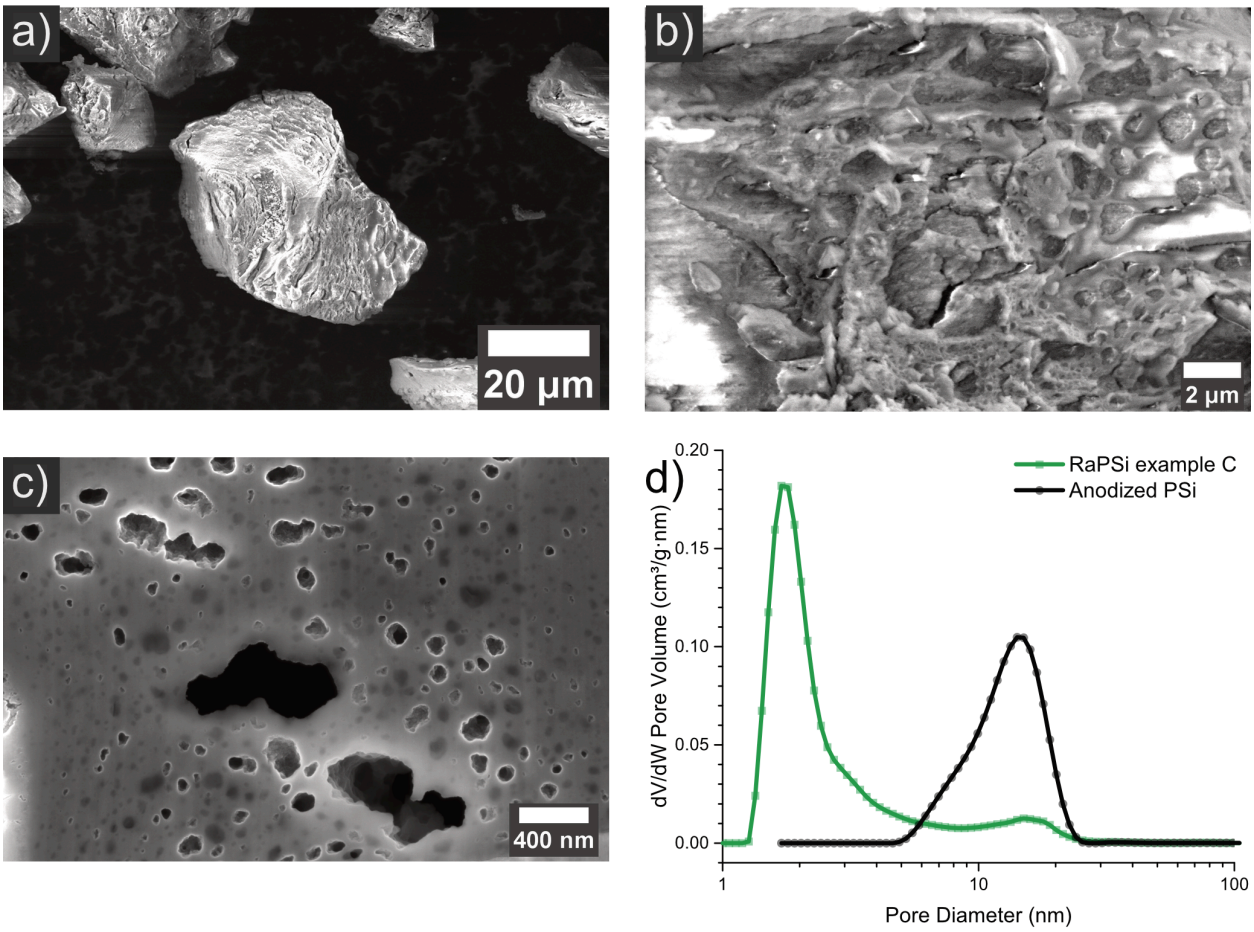

Figure S2.4. Representative SEM images obtained from a partially collapsed luminescent RaPSi samples with specific surface area (SSA) of 495 ± 7 m^2/g and pore volume of 0.44 ± 0.02 cm^3/g with (a) overall image of a RaPSi microparticle; (b) high magnification image from the surface of the particle and (c) high magnification image of the side wall of a FIB-cut slice through the particle. (d) Pore size distributions of the imaged RaPSi example particles with the respective initial anodized PSi.

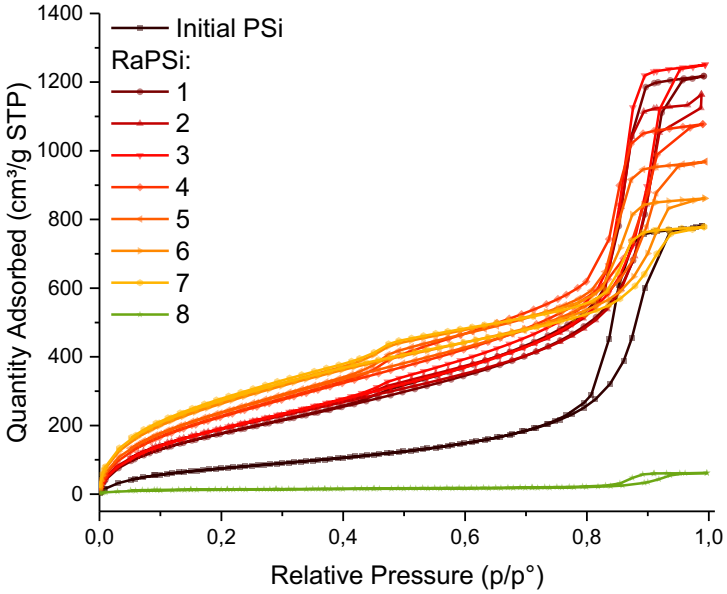

Figure S3. N_2 sorption isotherms of the initial anodized PSi and the RaPSi samples **1–8**.

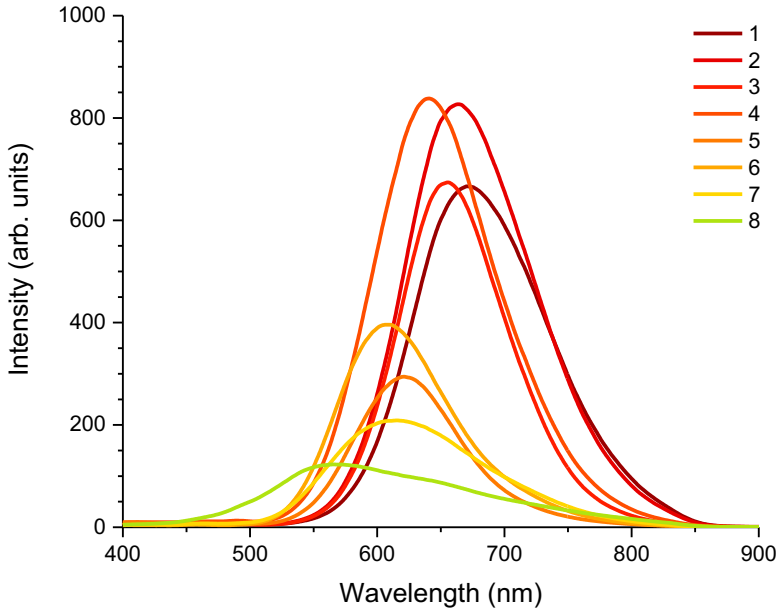

Figure S4. Non-normalized photoluminescence spectra of the RaPSi samples **1–8** excited at 325 nm. The spectra have not been weighted for e.g. different sample amounts.

Table S1. Peak wavelength and the apparent FWHM of the photoluminescence spectra obtained from the RaPSi samples **1–8**

Sample	**Peak wavelength (nm)**	**FWHM (nm)**	**PL color**
1	668	105	Red
2	660	102	
3	652	87	Orange
4	636	99	
5	616	83	
6	600	91	Yellow
7	605	118	
8	563	153	Green

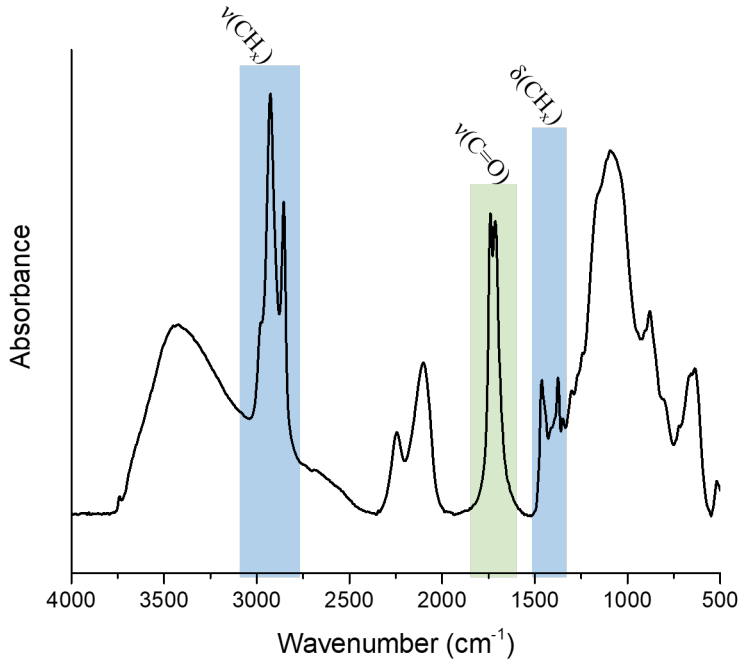

Figure S5. Photoacoustic FTIR absorbance spectra of COOH-RaPSi nanoparticles. The spectra confirms the presence of terminal –COOH -groups on the surface of the nanoparticles due to the carbonyl absorbance band located at ca. 1715 cm^{-1} and the alkyl chain stretching and bending bands at ca. 2900 cm^{-1} and 1460 cm^{-1}. The nanoparticles also show the presence of Si–O structures, as indicated by the broad stretching bands around 1050–1150 cm^{-1} and the bending vibration at 880 cm^{-1}, possibly due to the oxidation of the new surface formed during the milling of the nanoparticles.

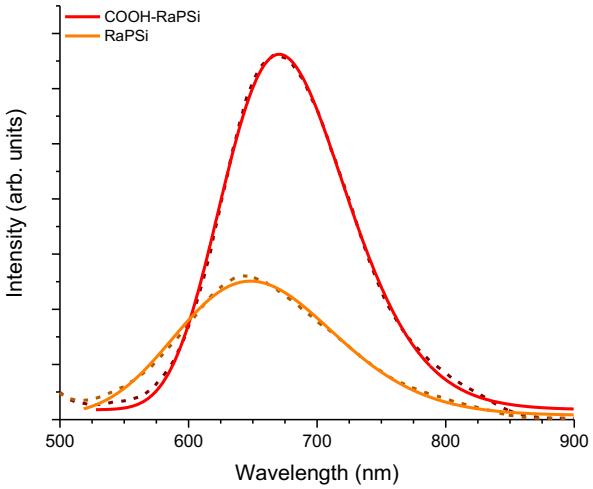

Figure S6. Photoluminescence spectra of RaPSi and the hydrosilylated COOH-RaPSi. The dashed lines present the raw data and the solid lines skewed Gaussian fittings. RaPSi nanoparticles for reference purposes were prepared by milling the non-functionalized microparticles in neat dodecane solution. For the analysis, the nanoparticles have been dispersed into distilled water with a concentration of 50 μg/mL. The excitation wavelength was 325 nm, with the emission side having a 390 nm cutoff filter. A redshift of 22 nm and intensity enhancement of a factor of 2 after the hydrosilylation is observed. The weaker PL of the non-functionalized RaPSi nanoparticles may be due to the introduced defects and partial oxidation during the milling process, while the hydrosilylated RaPSi appears less susceptible to the formation of such defects.

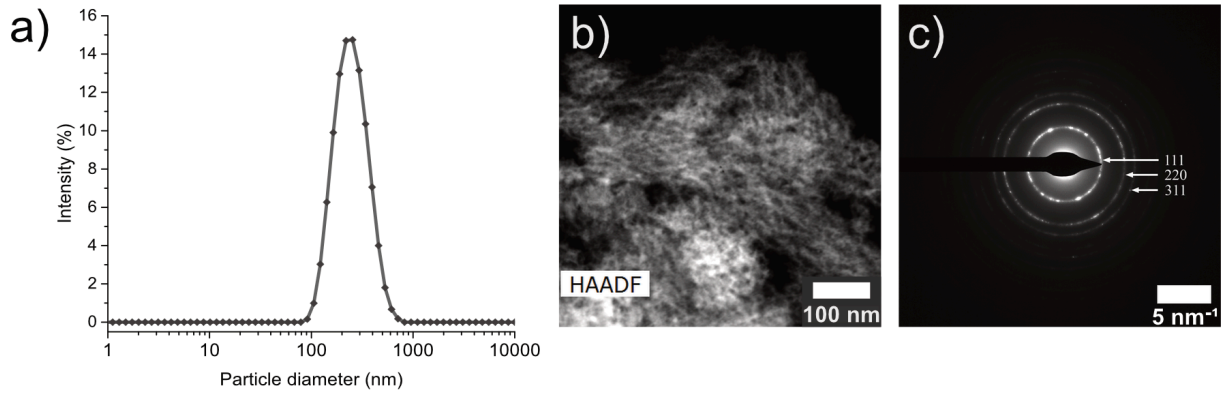

Figure S7. (a) Ball milling of COOH-RaPSi powder produces nanoparticles with a yield approaching 40% and a hydrodynamic diameter of 220 ± 8 nm and polydispersity index of 0.12. (b) STEM high-angle annular dark-field image of the COOH-RaPSi nanoparticles shows the characteristic fir-tree –like porous structure and the selected area electron diffraction pattern (c) indicates the particles retaining their crystallinity.

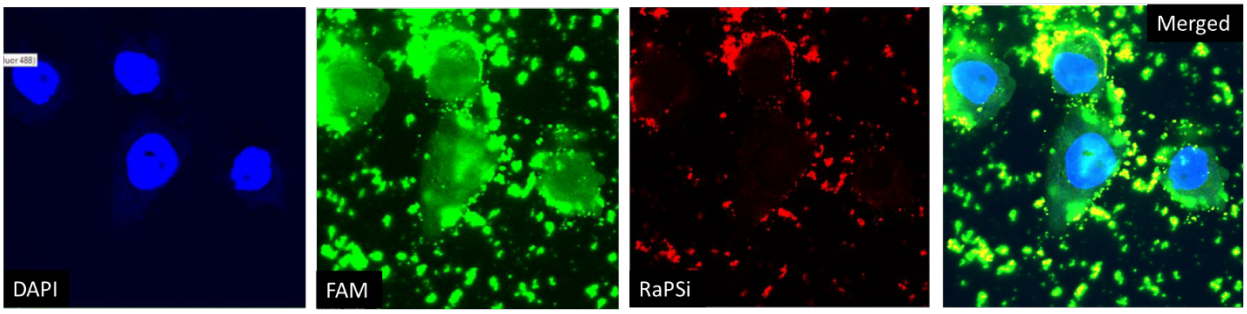

Figure S8. Confocal microscopy images of PPC-1 cells incubated for 1 h at 37 °C with FAM-RPARPAR modified COOH-RaPSi nanoparticles. Blue: DAPI-stained cell nucleus, Green: FAM, Red: RaPSi nanoparticles

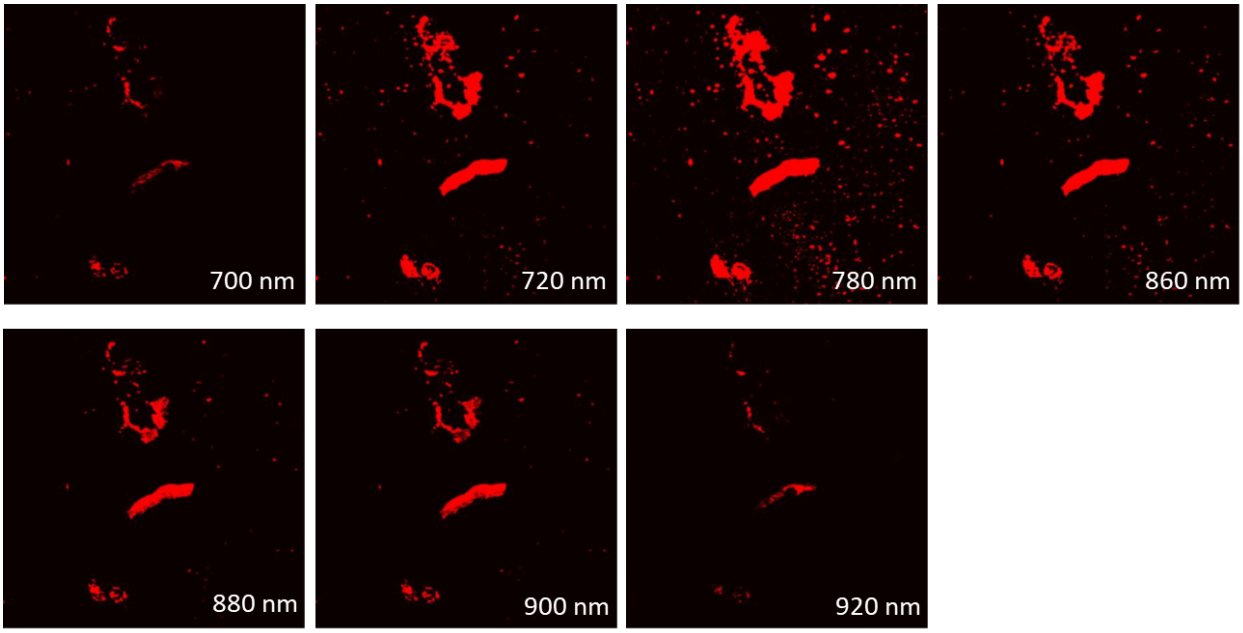

Figure S9. Confocal microscopy image of the excitation efficiency with 2-photon absorption of the COOH-RaPSi particles incubated with PPC-1 cells.

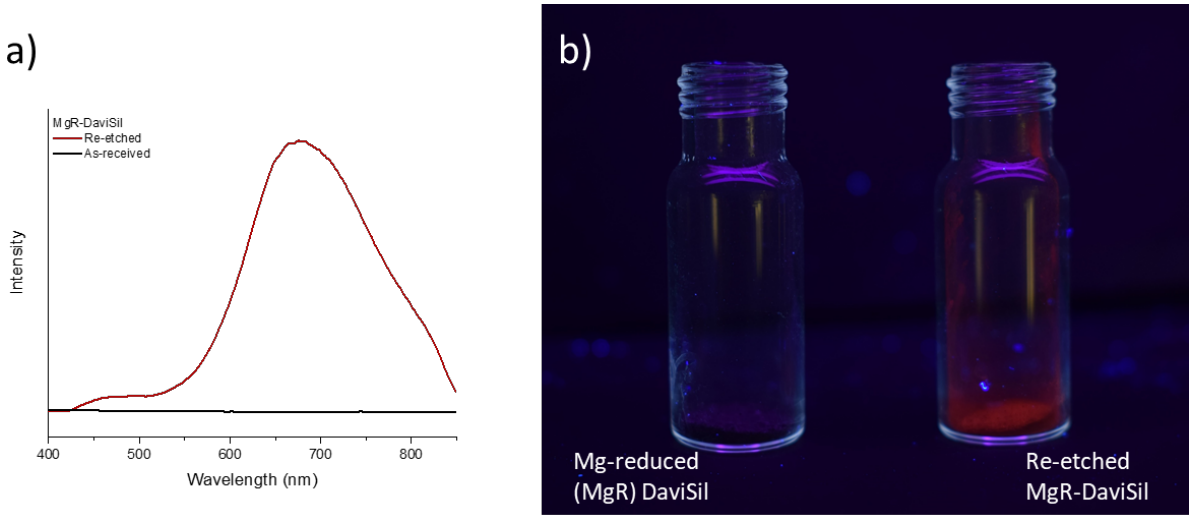

Figure S10.1. a) Photoluminescence spectra of the Mg-reduced DaviSil as received and as Re-etched. The excitation wavelength was 325 nm and a 390 nm long-pass filter was placed on the emission side. b) Photograph of the two types of particles under excitation by a handheld UV lamp set at 365 nm, taken with a DSLR, using 5 s exposure time.

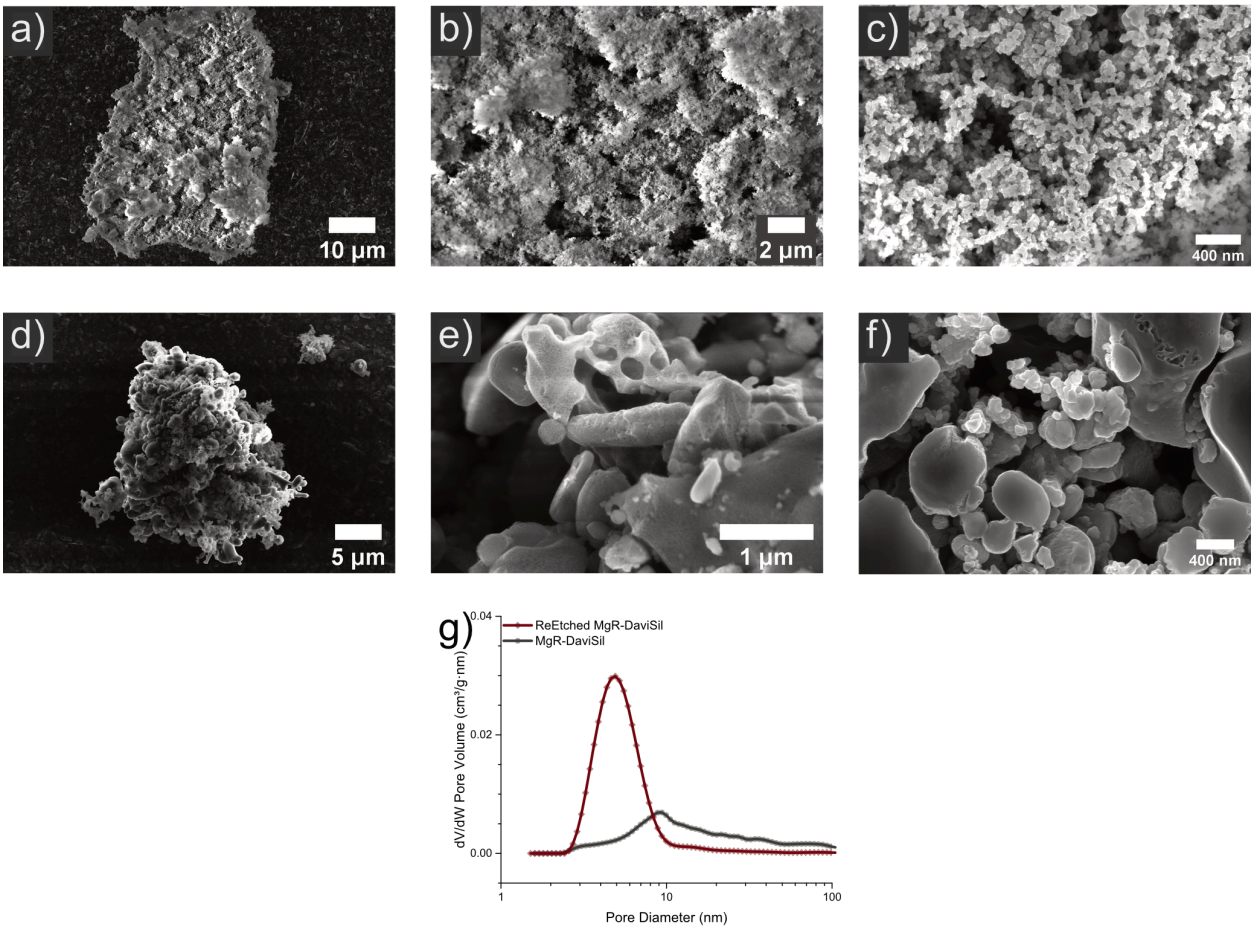

Figure S10.2. Representative SEM images obtained from as-received and ReEtched Mg-reduced (MgR) DaviSil samples where (a) and (d) present and overall image of a DaviSil particle before and after ReEtching, respectively. Similarly, (b) and (e) show a high magnification image of the particle surface with (c) and (f) presenting a high magnification image of the side wall of a FIB-cut slice through the particle. (g) Pore size distributions of the imaged DaviSil particles. The pore SSA and pore volume of the particles, before and after, were ca. 70 and 90 m^2/g and 0.26 and 0.13 cm^3/g, respectively. The low difference in SSA and the reduction of the pore volume after ReEtching suggests this particular MgR-DaviSil sample may have been overetched, and thus started to collapse. The structural collapsing is also suggested by the SEM images (d)-(f).